NANO LETTERS

2008
Vol. 8, No. 4
1257-1264

Development of the Tangential Mode in the Raman Spectra of SWCNT Bundles during Electrochemical Charging

M. Kalbac,*,†,‡ L. Kavan,† L. Dunsch,‡ and M. S. Dresselhaus§

J. Heyrovský Institute of Physical Chemistry, v.v.i., Academy of Sciences of the Czech Republic, Dolejškova 3, CZ-18223 Prague 8, Czech Republic, Leibniz Institute of Solid State and Materials Research, Group of Electrochemistry and Conducting Polymers, Helmholtzstrasse 20, D-01069 Dresden, Germany, and Department of Physics and of Electrical Engineering and Computer Science, MIT, Cambridge, Massachusetts 02139

Received November 28, 2007; Revised Manuscript Received January 21, 2008

ABSTRACT

The detailed analysis of the in situ Raman spectroelectrochemical behavior of single walled carbon nanotube (SWCNT) bundles is presented. The Raman modes of metallic SWCNTs exhibit striking changes even before the potential of the first van Hove singularity is achieved. Special attention has been paid to the development of the tangential (TG) mode broadening, which subsequently vanishes if the potential is shifted away from $V = 0$. The tangential mode band has been fitted by four components. During the electrochemical doping, three components of the tangential mode follow the predictions of a theoretical model for the LO modes of metallic tubes based on the Kohn anomaly. On the other hand, the behavior of the fourth component is consistent with a model based on electron−plasmon coupling. The TO mode of metallic tubes has been identified only at a doping level corresponding to 1.0 V or above. Our results also indicate an asymmetry in the behavior of the TG mode for positive electrode potentials relative to negative ones.

Raman spectroscopy is a frequently used spectroscopic method to investigate the state of single walled carbon nanotubes (SWCNTs) due to the resonant enhancement of their Raman signal. The main components of the spectra of SWCNTs are the radial breathing mode (RBM), the tangential displacement mode (TG), which is also known as the *G* band, the disorder-induced mode (*D*), and the high frequency two-phonon mode (*G′*).

The tangential displacement mode is observed in the region of 1450–1630 cm^{-1}. Group theory predicts six Raman-active lines in the TG mode region for chiral nanotubes: $2A_{1g} + 2E_{1g} + 2E_{2g}$, which are reduced to three Raman-active bands for zigzag and armchair tubes. However, the E_1 and E_2 modes have a much weaker Raman intensity than the totally symmetric A_1 modes.[1] Thus only two main components of the TG band are often considered in the analysis. They are usually referred to the G^+ and G^- lines, which are found at around 1590 and 1560 cm^{-1}, respectively. For semiconducting tubes, the G^+ line is attributed mainly to the diameter independent A_1^{LO} modes, while the G^- line is assigned to the A_1^{TO}. However, this interpretation has recently been revised for metallic SWCNTs due to the presence of a Kohn anomaly, arising from the electron–phonon interaction in metallic tubes.[2–4] The Kohn anomaly manifests itself as a sudden decrease of the phonon energy due to the change in the screening of the atomic vibrations by the conduction electrons. In metallic tubes, this can be the case, either for phonons with $q = 0$ or $q = K$, because the Fermi surface consists of only two points. Hence, the Kohn anomaly is suggested to have an important consequence for the A_1^{LO} mode of metallic tubes, and this mode is broadened and strongly softened to eventually lie below the frequency of the A_1^{TO} mode.[2–4]

In situ Raman spectroelectrochemistry is a well-established method to study the electronic structure of carbon nanostructures such as SWCNTs, DWCNTs (double walled carbon nanotubes), or fullerene peapods.[5–8,12] In contrast to chemical doping, electrochemistry allows the precise and well-controlled doping of carbon nanostructures. Recently, a number of spectroelectrochemical studies of SWCNTs have appeared in the literature that confirm the importance of spectroelectrochemistry for the evaluation of the electronic structure of carbon nanotubes.[9–12] Measurements on isolated individual tubes[13–15] seem to be preferable because the evaluation of the data is not disturbed by the overlapping of

* Corresponding author. E-mail: kalbac@jh-inst.cas.cz. Telephone: 420 2 6605 3804. Fax: 420 2 8658 2307.

† J. Heyrovský Institute of Physical Chemistry.

‡ Leibniz Institute of Solid State and Materials Research, Group of Electrochemistry and Conducting Polymers.

§ Department of Physics and of Electrical Engineering and Computer Science, MIT.

10.1021/nl073104h CCC: $40.75
Published on Web 03/01/2008

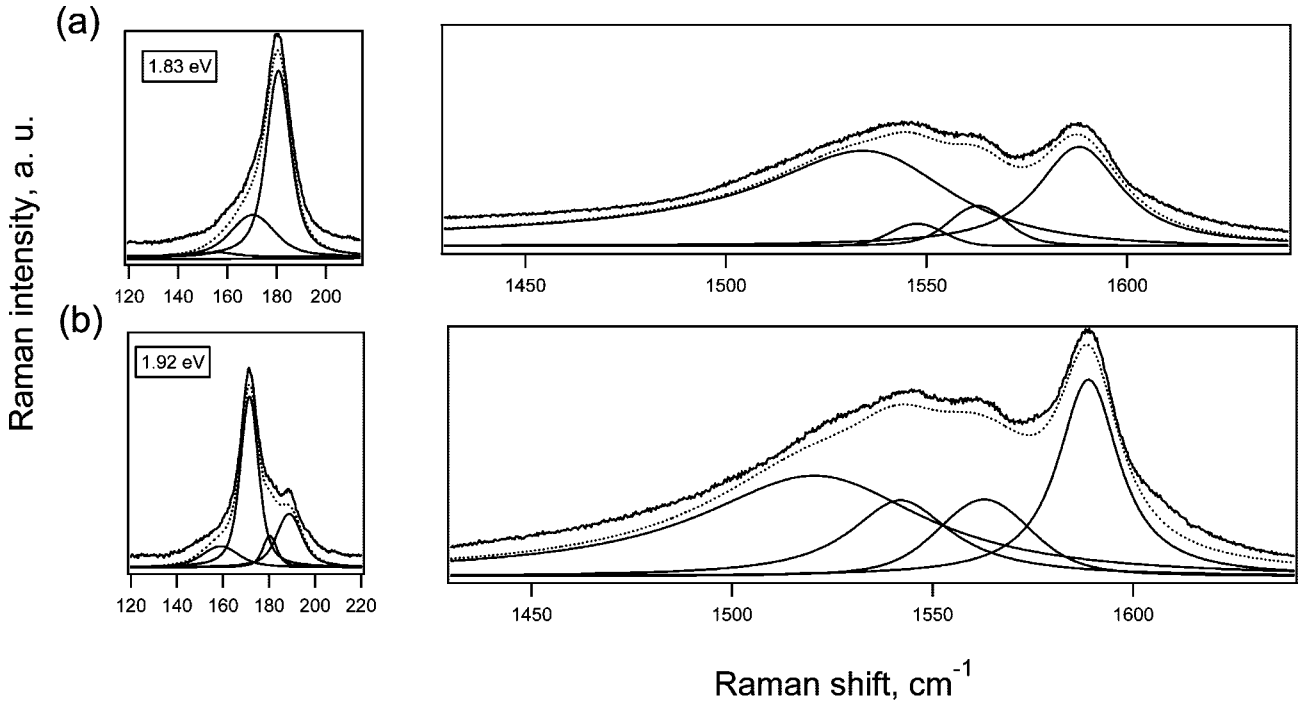

Figure 1. Raman spectra measured on SWCNTs and excited by 1.83 (top) and 1.92 eV laser energy (a). The spectra in the TG mode region (b) are fitted by three Voigt functions and one BWF line shape for both excitation energies. The RBM modes (on the left) are fitted by three and four Voigt functions for 1.83 and 1.92 eV, respectively. The dotted curves correspond to a sum of the fitted components. For clarity, the original measured spectra are slightly offset from the sum of the fitted components. The intensity scale in the figure is the same for the spectra excited by the same laser energy.

signals coming from several tubes. On the other hand, the effects resulting from the bundling of SWCNTs are then not observed.

In the present work, we inspect the Raman spectra of metallic tubes in SWCNT bundles during electrochemical doping. Precise control of the electrochemical charging enabled us to follow the detailed development of the TG mode of SWCNT bundles regarding its dependence on the electrode potential. To follow the effect of electrochemical charging on the lower component of the TG mode in SWCNT bundles, we use a thin SWCNT film with a narrow diameter distribution of the SWCNTs on a Pt electrode. The narrow diameter distribution ensures that by using a certain laser excitation energy, nanotubes with only a few different (n,m) chiralities are in resonance at the same time. Recently it was suggested that the broadening in the Raman spectra of metallic tubes can be fully explained by the Kohn anomaly.[4] However, we show here that the Raman spectra of SWCNT bundles are more complex. In particular, the development of the lowest frequency G^- component of the TG mode of metallic tubes in SWCNT bundles during electrochemical doping does not follow the predictions of the Kohn anomaly. We present new arguments supporting the explanation of the broadening of G^- in metallic tubes in bundles based on the electron−plasmon coupling mechanism. Therefore, to fully explain the TG mode of metallic tubes in bundles, both the Kohn anomaly effect and the effects resulting from bundling, such an electron−plasmon coupling, must be considered.

Figure 1(a) and Figure 1(b), respectively, show the RBM and G^- band in Raman spectra of SWCNTs excited by 1.83 and 1.92 eV laser radiations. The Raman spectra in the RBM region are fitted using Voigt functions. The positions of the most intense RBM bands are at about 180 cm^{-1} for 1.83 eV laser excitation energy and 172 cm^{-1} for 1.92 eV laser excitation energy. The diameter of SWCNTs can be approximated by the simple equation $\omega_{RBM} = A/d_t + B$ where $A = 217.8$ and $B = 15.7$.[16] Hence the RBM mode positions of the most intense bands correspond to the tube diameters of 1.32 and 1.26 nm for 1.92 and 1.83 eV laser excitation energies, respectively.

The Raman spectra of SWCNT bundles in the TG region were fitted by four lines. The attempts to fit all lines by Voigt functions failed as it was not possible to achieve a reasonable agreement between the fitted and experimental data. Finally, one BWF line and three Voigt functions have been successfully used to fit the experimental data.

For 1.83 eV excitation, the three Voigt modes are centered at 1588, 1562, and 1547 cm^{-1} in the Raman spectra of SWCNTs in the TG mode region. The BWF line is centered at 1534 cm^{-1}. Recently, Das et al.[17] studied a sample of SWCNT bundles with a similar diameter distribution using 1.96 eV laser excitation. In this case, the TG mode spectra were fitted by three Lorentzians (L1–3) at 1540, 1567, and 1590 cm^{-1}, which were, respectively, assigned to the LO mode of metallic tubes (L1), a combination of the LO mode of metallic tubes and the TO mode of semiconducting tubes (L2), and the combination of the TO mode of metallic tubes and the LO mode of semiconducting tubes (L3). Interestingly the authors did not use the BWF line shape. Except for the additional fourth BWF band at 1534 cm^{-1}, the positions of the bands found by the authors in ref 17 correspond well to

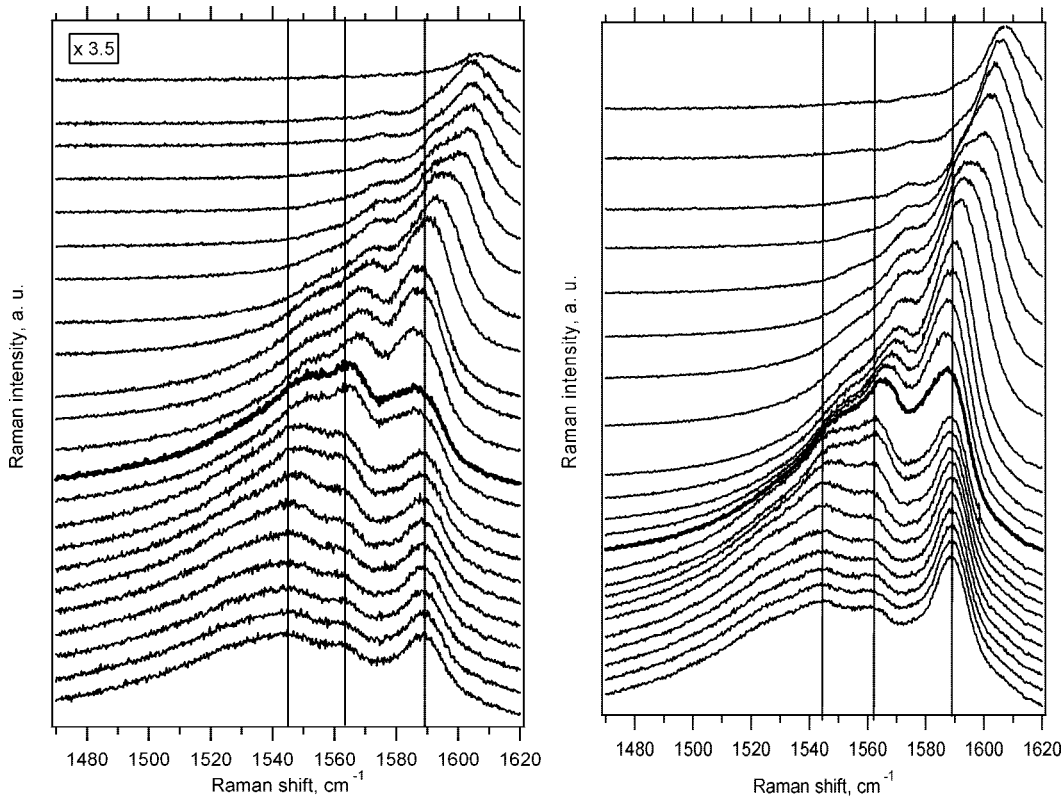

Figure 2. In situ Raman spectroelectrochemical data on SWCNTs in SWCNT bundles in the electrode potential range from 0 to 1.5 V (from bottom to top). The spectra are excited by 1.83 eV (left panel) and 1.92 eV (right panel) laser radiation. The bold line corresponds to an electrode potential of 0.5 V. The electrochemical potential change between adjacent curves in the figure is 0.05 V from 0 to 0.7 V and then 0.1 V in going from 0.7 to 1.5 V. The spectra are offset for clarity, but the intensity scale is the same for all spectra in their respective windows. The vertical solid lines are a guide to the eye and correspond to the position of the various phonon features at 0 V.

the positions of the bands in our work. The low frequency band with a BWF line shape is found at both excitation energies of 1.83 and 1.92 eV (Figure 1). This behavior thus is not a consequence of any unique behavior of special tubes. Because the position of the G^- mode in isolated metallic tubes is usually above 1540 cm^{-1};[1518] we attribute the additional broadening of the G^- band for metallic tubes to a phonon−plasmon coupling due to the bundling effect. This assignment is in accord with previous studies.[1,19–21]

The detailed experimental in situ Raman spectroelectrochemical data on SWCNT bundles for anodic potentials are shown in Figure 2. The spectra are excited by 1.83 eV (left panel) and 1.92 eV (right panel) laser energy. Several attempts were made to fit the spectra in Figure 2 during the electrochemical doping process. It was, however, found that the phonon bands change their position, shape, intensity, and width by electrochemical doping, and therefore all these parameters were fitted for each potential. This approach resulted in severe problems with the fitting procedure because there are several different combinations of fitting parameters that give a similar fit quality. Therefore, the original spectra are presented here rather than showing plots of the fitted parameters.

Figures 2 and 3 show the overall bleaching of the spectra during electrochemical doping. This is the most obvious change, and it is attributed to the filling/depleting of the van Hove singularities. However, there are many other changes in these spectra as a function of the applied potential. There is the narrowing of the G^- component of the TG mode (at 1547 and 1562 cm^{-1} in Figure 2) in going from electrode potentials of 0 V to 0.5 or −0.5 V. This effect has been recently attributed to the Kohn anomaly, which is quenched as the electrochemical potential is increased. The electrochemical charging leads to a change of the Fermi level position and subsequently the electronic states are filled or depleted with electrons. The depletion of electron charge is believed to decrease the electron–phonon coupling. Thus the line broadening associated with electron–phonon coupling should be suppressed by the application of an electrochemical potential. Indeed, the broadening of the G^- band assigned predominately to the LO mode of metallic tubes is reduced by increasing the electrode potential.

A more detailed analysis of the development of the Raman spectra in Figure 2 measured in situ during electrochemical doping points to several other changes. In particular, the change of the position of the G^+ mode is very interesting. At the beginning of the electrochemical doping, this band moves to lower frequencies but subsequently (with the increase of the electrode potential) it again shifts to higher frequencies. The maximum downshift in frequency is 3.5 cm^{-1} for the 1.83 eV excitation, and it is achieved at an electrode potential of 0.55 V. Increasing the potential to 1.5 V leads to a final upshift of 17 cm^{-1} with respect to the position of the G^+ at 0 V. The development of this mode is

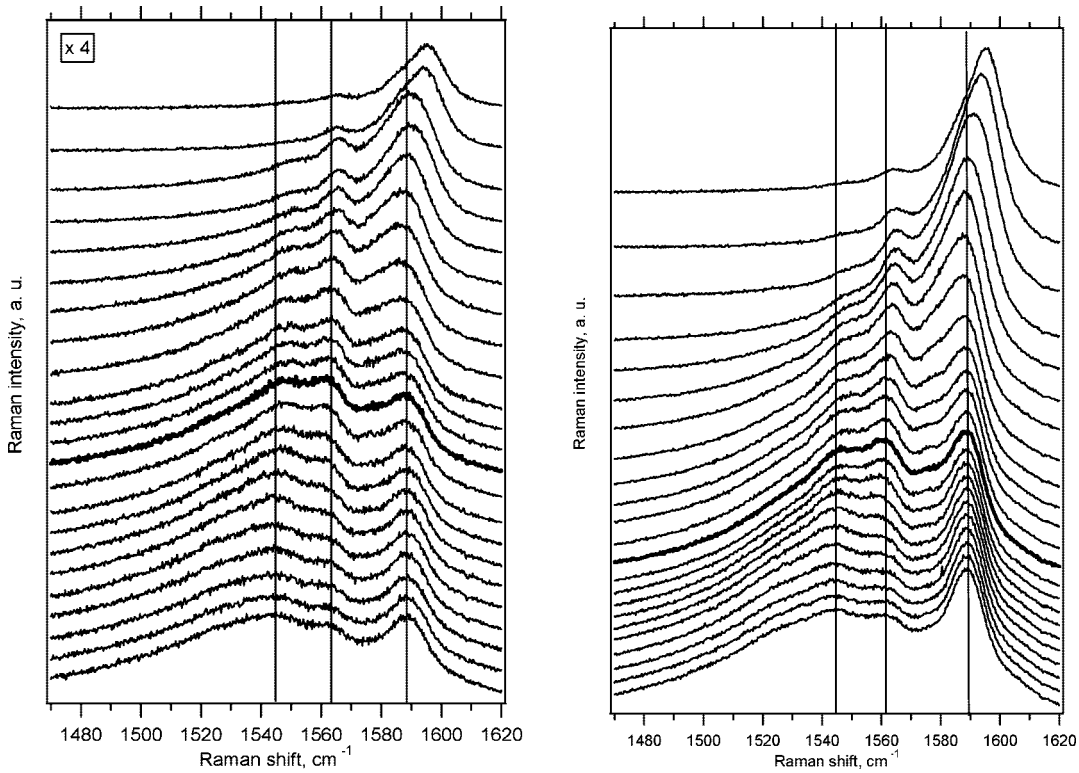

Figure 3. In situ Raman spectroelectrochemical data on SWCNTs in the range from 0 to −1.5 V (from bottom to top). The spectra are excited by the 1.83 eV (left panel) and 1.92 eV (right panel) laser lines. The bold line corresponds to an electrode potential of −0.5 V. The electrochemical potential has been changed by 0.05 V for electrode potentials from 0 to −0.7 and then by 0.1 V to the final potential of −1.5 V. The spectra are offset for clarity, but the intensity scale is the same for all spectra in their respective windows. The vertical solid lines are a guide to the eye, and they correspond to the position of bands at an electrode potential of 0 V.

slightly different for the 1.83 and 1.92 eV laser excitation. The maximum downshift of the frequency for the 1.92 eV excitation is 2 cm^{-1}, and it is achieved also at an electrode potential of 0.55 V. The position of the G^+ mode at the maximum electrode potential (1.5 V) is by 18.5 cm^{-1} higher than that at 0 V for the 1.92 eV laser radiation.

The band at around 1560 cm^{-1} does not change its position at the beginning of the doping, e.g., from 0 to 0.5 V. However, there is an abrupt upshift of this band at an electrode potential of 0.55 V. The band is subsequently further upshifted with an increasing potential until it reaches the value of 1575 cm^{-1} at 0.9 V. As the electrode potential increases beyond 0.9 V, this mode seems to maintain its maximum frequency, but it is difficult to follow the band position due to a strong monotonic decrease of its intensity. However, the development of the intensity of this mode is nonmonotonic. First, there is an increase in intensity (for potentials from 0 to 0.5 V), while at 0.5 V, this band reaches its maximum intensity, for an electrode potential at about 0.5 V and above, the band again bleaches.

The band at around 1547 cm^{-1} is difficult to resolve at electrode potentials higher than 0.55 V. Nevertheless, it seems that it moves up in frequency as the electrode potential increases. The development of the band intensity is nonmonotonic. The maximum intensity of this band is found at a potential around 0.4 V.

The last band at 1534 cm^{-1} fitted by the BWF line shape (Figure 1) is difficult to resolve even if no electrode potential is applied. Therefore, the development of its position during electrochemical doping can not be precisely followed. Nevertheless, the band exhibits a strong decrease in intensity (starting at about 0.15 V) and it almost completely vanishes at a potential of 0.5 V.

The effects described above are very similar for both excitation energies (1.83 and 1.92 eV). As shown by the radial breathing modes in Figure 1, the tubes with different diameters are in resonance for the two excitation energies. Hence, there is no strong chirality or diameter dependence of the behavior of the TG mode during electrochemical charging. Furthermore, these data demonstrate the robustness of the phenomena expected for samples with a slightly different diameter distribution.

Figure 3 shows the detailed in situ Raman spectroelectrochemical data for SWCNT bundles at cathodic potentials. The spectra are excited by the 1.83 eV (left panel) and 1.92 eV (right panel) laser energy. The development of the spectra is similar as compared to the spectra in Figure 2 for anodic doping. However, a more detailed analysis shows several differences. Probably the most distinct effect is the development of the frequency of the G^+ mode. There is a much smaller downshift of the G^+ mode at the beginning of doping. The maximum downshift is found at a higher electrode potential than in the case of a positive doping. The maximum of the G^+ mode upshift at −1.5 V is only 6 cm^{-1} for the 1.83 eV excitation and 7 cm^{-1} for the 1.92 eV laser excitation, which corresponds to just $^1/_3$ of the upshift

observed at the corresponding anodic potential (1.5 V). One can argue that the negative doping can be less effective or that the zero level of the Fermi energy is shifted to negative potentials. This argument would be supported by a slower bleaching of the G^+ mode during the negative doping compared to the positive doping procedure. The "slower bleaching" could explain the asymmetry of the effect for about 0.1–0.2 V in the potential range. (The observed behavior in the intensity of the spectrum at an electrode potential of −1.5 V in Figure 3 matches the corresponding behavior of the intensity of spectra between potentials of 1.3−1.4 V in Figure 2.) However, the shift of the G^+ mode at a potential of −1.5 V corresponds to the shift at an anodic electrode potential of +0.8 V. The asymmetry in the potential scale would then be of 0.7 V, which is far above the expected value. Furthermore the "potential correction" would just broaden the kink observed in the development of the frequency of the G^+ mode at 0.5 V in the anodic range but would not account for the magnitude of this effect. In other words, the value of the minimum frequency of the G^+ mode would be the same for both the anodic and cathodic doping. However, the minimum frequency will only be reached at higher potentials for negative doping than for positive doping.

There is also a difference in the behavior of the mode at 1560 cm^{-1} because its upshift for cathodic doping (Figure 3) is less pronounced compared to that for anodic doping in Figure 2. Furthermore, the band can be followed up to potentials of −1.5 V. It seems that its frequency reaches a maximum at a potential around −1.2 V and then the band again moves to lower frequencies.

The band at 1547 cm^{-1} also exhibits an asymmetric bleaching, and thus a small upshift can be followed at electrode potentials above −0.5 V.

Finally the broad BWF band at 1534 cm^{-1} seems to resemble the behavior during anodic doping; it bleaches at the same potential, around −0.5 V.

We have shown previously that an extensive doping of SWCNTs leads to a strong decrease in the intensity of the Raman signal. It is assumed that the change of the TG mode intensity is connected to the change of the resonance condition. The intensity of Stokes resonant Raman scattering (I) is given by:

$$I = \frac{c}{|(E_L - E_{ii} - i\gamma)(E_L + E_{ph} - E_{ii} - i\gamma)|^2} \qquad (1)$$

where E_L is laser photon energy, E_{ii} the optical transition energy, E_{ph} the phonon energy, and γ is the damping constant. Typical values for RBM are $E_{ph} \approx 0.02$ eV and $\gamma \approx 0.05$ eV. The c term in the numerator includes the electron–phonon matrix elements.

As mentioned previously, the electrochemical charging of SWCNTs leads to a shift of the Fermi level. As soon as the Fermi level reaches the energy of the van Hove singularity, it changes the filling of the vHS and thus suppresses the electronic transitions from/to this particular singularity. If the Raman signal is in resonance with such a singularity, a strong bleaching of the Raman intensity for that feature is expected. Now, let us assume that the setting of the potential at 0 V roughly corresponds to the position of the Fermi level in the middle between the singularities. In the present experiments, the level of the respective van Hove singularity is around 0.9 eV. (For example, the spectra on the left panel of Figure 2 are excited by 1.83 eV laser radiation. Therefore, only those SWCNTs with an energy difference between the van Hove singularities close to 1.83 eV are in resonance, and thus their features appear in the Raman spectra.) Assuming that the change of the electrode potential by 1 V leads to the Fermi level shift by 1 eV, the energy level of the particular van Hove singularity should be reached at a potential of about 0.9 V. In other words, one would expect a strong change in the Raman signal when the electrode potential of 0.9 V is reached. Indeed, there is strong bleaching of the spectra, which is most obvious at around 0.9 V. Nevertheless, there are already significant changes in the intensity and shape of the spectra as early as when a potential of 0.15 V is applied. Thus even small changes in the electrochemical potential, far below the van Hove singularity, cause serious changes in the electronic structure of the metallic SWCNTs. The Raman spectra are consequently changed. Recently, some changes in the shape and frequency of the LO mode of individual metallic SWCNTs have been interpreted in terms of a Kohn anomaly.[4] However, our data here show that the Kohn anomaly does not fully explain the common assignment of the Raman features of metallic tubes in the TG mode region of the spectra of SWCNT bundles. For example, the G^+ mode for bundled tubes has been assigned to a combination of the LO mode of the semiconducting SWCNTs and the TO mode of the metallic tubes. However, the change of phonon energy of the G^+ mode at 1590 cm^{-1} during the electrochemical doping rather resembles the predictions for the shift of the LO mode of metallic tubes induced by doping[4] because it downshifts by a few cm^{-1} at potentials between 0.4 and 0.65 V at first and then upshifts by nearly 20 cm^{-1} at potentials between 0.7 and 1.5 V (Figure 2). The assignment of this band to the TO mode of metallic tubes should be excluded because the position of this mode should not change with a shift of the Fermi level. Because the behavior of the G^+ mode during the electrochemical doping in our spectra follows the predictions of the Kohn anomaly theory for the LO mode and not for the TO mode, we suggest the assignment of this mode to the LO mode of metallic tubes. The previous assignment of the G^+ band to the LO mode of semiconducting tubes by Das et al.[17] is not favorable in our case due to the following reasons: (1) The semiconducting nanotubes in our samples (the diameter range between 1.2–1.6 nm) are not in resonance with laser excitation energies of 1.83 nor 1.92 eV. (2) Avouris et al. recently showed[22] that the frequency of the G^+ mode of semiconducting tubes increases monotonically with increasing potential, i.e., no "kink" in the G^+ mode frequency dependence on potential, as is observed in the present work, is expected. This reference shows the effect to be valid for both the LO and TO mode of semiconducting SWCNTs and to favor large diameter tubes ($d \approx 2.4$ nm).[22] For smaller diameter tubes, the effects are weaker. Nevertheless, these effects should still be visible

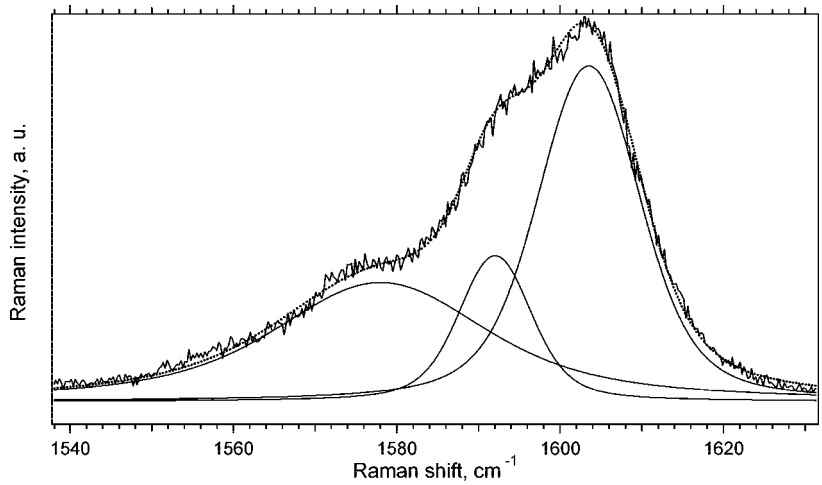

Figure 4. Raman spectra measured on SWCNT bundles excited by 1.83 laser energy at an electrode potential of 1.1 V. The spectrum is fitted by three Voigt functions with a frequency at 1576, 1592, and 1605 cm^{-1}. The dotted curve corresponds to a sum of the fitted components.

for tubes with a diameter of 1.5 nm,[22] which is close to the diameter of tubes used in our study.

The behavior of the other Raman features at 1562 and 1547 cm^{-1} during electrochemical doping excludes their assignment to the TO mode of metallic tubes. On the other hand, it does not exclude their assignment to the LO mode of metallic tubes. The Raman features at 1562 and 1547 cm^{-1} found in the spectra of SWCNTs are broader (for the 1.83 eV laser radiation, the FWHM for these features is 27 and 30 cm^{-1}, respectively, as seen in the fit in Figure 1) than the feature at 1590 cm^{-1} (where the FWHM is 18 cm^{-1} for the 1.83 eV laser radiation, Figure 1). The broadening of these two bands would explain why the shifts of the bands are not resolved unless their widths are reduced by electrochemical doping. It was shown recently,[18] that the broadening of the TO mode of metallic tubes is strongly dependent on their chirality. While the armchair tubes exhibit a very weak broadening, the zigzag tubes show a very strong broadening.[18] The magnitude of the broadening is also related to the magnitude of the downshift of the LO mode for a given metallic tubes. The strongest downshift is observed for the most broadened bands.[18] This is not surprising because a stronger electron–phonon coupling would lead to a stronger Kohn anomaly effect, e.g., to a larger frequency downshift. Thus the tubes with different (*n,m*) values would have a different frequency of the LO mode and the multiple LO modes can be found in the experimental spectra of SWCNT bundles. In other words, on the basis of the discussion above, the observed development of all features at 1547, 1562, and 1590 cm^{-1} in the TG mode region with changing electrode potential favor their assignment to the LO modes of metallic tubes with different chiralities.

Recent study of metallic tubes has shown that the G^- band upshifts by almost 50 cm^{-1} if the Fermi level is shifted from 0 to −0.6 V.[15] A simultaneous narrowing of the G^- band results in an increase in the intensity of the mode by a factor of 2−3. The effects of electrochemical doping of SWCNT bundles are in the same direction, but they are not as strong as in the case of individual tubes. The electron–phonon coupling has a different strength for tubes with different (*n,m*) values;[18,23] however, there is a large number of nanotubes contributing to the spectra of nanotube bundles. Therefore, even the extreme behavior of an individual SWCNT in the bundle with a particular (*n,m*) value does not cause strong changes in the overall shape of the TG mode in the spectra of SWCNT bundles. Furthermore, the intertube interactions can be responsible for an additional weakening of the effects caused by the Kohn anomaly.

The results of this study show that a new band at 1592 cm^{-1} appears in the Raman spectra at electrode potentials of 1.0 V. The new band is more pronounced in the spectra excited by 1.83 eV laser radiation (Figure 2 and the fit shown in Figure 4). This band does not exhibit any change in frequency with changing potential, which would favor its assignment to the TO mode for metallic tubes. This assignment would be consistent with the development of a phonon frequency of the TO and LO modes of the metallic tubes during charging. In other words, in the Raman spectra of undoped metallic tubes, the weaker TO mode is not resolved in the presence of the much stronger LO mode of metallic tubes. However, in the Raman spectra of doped metallic tubes, the LO mode is upshifted, while the TO mode does not change its position, and hence it can be observed in the spectra as a new band at 1592 cm^{-1}.

The band with the BWF line shape is the feature that exhibits the fastest monotonic bleaching with changing electrode potential. There is neither an enhancement of its intensity nor is there a significant change in its peak frequency. This contrasts with the behavior of modes at 1547, 1562, and 1590 cm^{-1}. In fact, on the basis of previous results,[18] one would expect even more pronounced changes of the band with the BWF line shape as a function of electrode potential than for the other TG mode features. Because the band at 1534 cm^{-1} has the lowest frequency and it is the broadest, we would expect to observe the following behavior for this Raman band: (1) the electron–phonon coupling should be the strongest, (2) the doping should result in a remarkable simultaneous narrowing and a

shift to higher frequencies, (3) the line shape of the band should be unaffected at a low doping level, and (4) a strong increase in the intensity of the band at 1534 cm^{-1} during the electrochemical doping process. Obviously these effects are contradictory to the experimental observation. Thus our experimental results indicate a different origin of the BWF line than the Kohn anomaly. We therefore interpret our observations as consistent with its previous assignment to a phonon−plasmon coupling in SWCNT bundles.[20] The fast bleaching of the latter band with increasing electrode potential indicates that the phonon−plasmon coupling in SWCNT bundles is more sensitive to the shift of the Fermi level than in the broadening of the LO modes of individual metallic tubes due to an electron−phonon coupling.

In conclusion, we studied the development of the TG mode of metallic tubes during the electrochemical doping in detail. It was found that the assignment of the TG mode features is more complex than that given by the previous description of the development of the spectra during electrochemical charging. In particular, the assignment of the G^+ mode to a combination of the TO mode of metallic tubes and the LO mode of semiconducting tubes does not adequately account for the observed behavior of the G^+ mode during the electrochemical charging. As shown here, the G^+ mode is softened in going from a potential of 0 to 0.5 V and is subsequently hardened in changing the potentials from 0.5 to 1.5 V. This behavior is characteristic for the LO mode of metallic tubes. The behavior of other modes fitted by the Voigt function also indicates an assignment of the G^+ feature to the LO modes of metallic tubes. The different frequencies of the LO modes correspond to tubes with a different strength of electron–phonon coupling. We believe that the TO mode of metallic tubes is not resolved in the spectra of nondoped SWCNT bundles. However, it can be found at around 1592 cm^{-1} in the spectra for SWCNT bundles if a potential of 1.0 V or higher is applied. In contrast to the behavior of the LO modes fitted by Voigt functions, the BWF line exhibits a monotonic bleaching during electrochemical doping and thus it is attributed to a phonon−plasmon coupling mechanism in SWCNT bundles.

The BWF line shape can be found also for metallic inner tubes of DWCNTs in bundles.[24] In this case, the inner tubes do not interact with other neighboring tubes in a bundle but they interact with the outer tube shell. However, the evaluation of the effects of the doping is more complex because the inner tube is shielded by outer tube shell[25] and thus more experimental data are required to get a correct interpretation of this problem.

A more detailed analysis of the positive and negative doping of SWCNT bundles shows several differences. There is a much smaller downshift of the G^+ mode at the beginning of negative doping than in the case of positive doping. Furthermore the maximum of the G^+ mode upshift at −1.5 V corresponds to only $^1/_3$ of the upshift observed at an electrode potential of +1.5 V.

In general, one should not exclude the possibility that these differences in behavior could be caused by different ions that are employed in the anodic and cathodic doping for balancing the charge at the nanotube upon doping. However, it was shown that only electrolytes with bulky cations, like ionic liquids, have a significant influence on doping behavior.[26] We also assume that in the range of potentials where the major changes of the G^- component of the TG mode occur, the compensating ions are located mostly on the surface of nanotube bundles or inside the interstitial voids within the nanotube bundles (at higher electrode potentials).[27] Thus the observed effects should not be related to the insertion of ions inside a hollow space of SWCNTs. Nevertheless, this is still an open issue and more detailed studies on SWCNT bundles of different sizes are needed.

The considerable differences during positive and negative doping can be used for analytical purposes because negative and positive doping can be distinguished experimentally. However, the observed effects are probably even more important for theory. Up to now, most of the studies of carbon nanotubes assume that the singularities are symmetrical with respect to some central energy as it is also assumed for graphene, from which nanotubes are derived. The data presented here show that this assumption requires more careful investigations.

Experimental. Single walled carbon nanotubes (SWCNTs) were available from our earlier work.[28] Briefly, the SWCNTs were prepared by laser ablation[29] using a Ni/Co catalyst and purified by reflux in 15% H_2O_2, which was followed by washing with HCl to remove residual catalyst.[30] The electrodes for in situ spectroelectrochemical studies were fabricated by the evaporation of a sonicated ethanolic slurry of SWCNTs on Pt electrodes. The film was outgassed at 80 °C in vacuum and then mounted in the Raman spectroelectrochemical cell. The spectroelectrochemical cell was airtight and had a single compartment and was equipped with a glass optical window for spectroscopic measurements.

The cell was assembled in a glovebox (M. Braun); the glovebox atmosphere was N_2 containing <1 ppm of both O_2 and H_2O. Electrochemical experiments were carried out using PG 300 (HEKA) or 273A (EG&G PAR) potentiostats with Pt auxiliary and Ag wire pseudoreference electrodes, the electrolyte solution was 0.2 M $LiClO_4$ + acetonitrile (both from Aldrich; the latter dried by 4 Å molecular sieve).

The Raman spectra were excited by Ar^+, Kr^+ lasers (Innova 300 series, Coherent), and by a Ti-sapphire laser (899LC, Coherent). Spectra were recorded by a T-64000 spectrometer (Instruments SA) interfaced to an Olympus BH2 microscope (objective 50×). The laser power impinging on the cell window or on the dry sample was between 1 and 5 mW. The spectrometer was calibrated by the F_{1g} mode of Si at 520.2 cm^{-1}.

Acknowledgment. This work was supported by the Academy of Sciences of the Czech Republic (contract no. KJB400400601), GACR (contract no. 203/07/J067) and by the Czech Ministry of Education, Youth and Sports (contract no. LC-510). M. Kalbac acknowledges funding by the Alexander von Humboldt Society. M. S. Dresselhaus acknowledges support from NSF/DMR-07-04197. The authors kindly acknowledge the discussion with Prof. Kris Kempa

from Boston College and Prof. Jing Kong and Hootan Farhat from MIT, Cambridge, MA.

References

(1) Brown, S. D. M.; Jorio, A.; Corio, P.; Dresselhaus, M. S.; Dresselhaus, G.; Saito, R.; Kneipp, K. *Phys. Rev. B* **2001**, *6315*, 155414-1–155414-8.

(2) Piscanec, S.; Lazzeri, M.; Mauri, F.; Ferrari, A. C.; Robertson, J. *Phys. Rev. Lett.* **2004**, *93*, 185503-1–185503-4.

(3) Lazzeri, M.; Piscanec, S.; Mauri, F.; Ferrari, A. C.; Robertson, J. *Phys. Rev. B* **2006**, *73*, 155426-1–155426-6.

(4) Piscanec, S.; Lazzeri, M.; Robertson, J.; Ferrari, A. C.; Mauri, F. *Phys. Rev. B* **2007**, *75*, 035427-1–035427-22.

(5) Kalbac, M; Kavan, L.; Zukalova, M; Dunsch, L. *NANO* **2007**, *1*, 219–227.

(6) Kalbac, M; Kavan, L.; Zukalova, M; Dunsch, L. *J. Phys. Chem. C* **2007**, *111*, 1079–1085.

(7) Kalbac, M; Kavan, L.; Zukalova, M; Dunsch, L. *Chem.—Eur. J.* **2006**, *16*, 4451–4457.

(8) Kavan, L.; Kalbac, M; Zukalova, M; Dunsch, L. *J. Phys. Chem. B* **2005**, *109*, 19613–19619.

(9) Rafailov, P. M.; Thomsen, C. *J. Optoelectron. Adv. Mater.* **2005**, *7*, 461–464.

(10) Corio, P.; Jorio, A.; Demir, N.; Dresselhaus, M. S. *Chem. Phys. Lett.* **2004**, *392*, 396–402.

(11) Rafailov, P. M.; Maultzsch, J.; Thomsen, C.; Kataura, H. *Phys. Rev. B* **2005**, *72*, 045411-1–045411-7.

(12) Kavan, L.; Dunsch, L. *ChemPhysChem* **2007**, *8*, 975–998.

(13) Okazaki, K.; Nakato, Y.; Murakoshi, K. *Phys. Rev. B* **2003**, *68*, 035434-1–035434-5.

(14) Wang, Z. J.; Pedrosa, H.; Krauss, T.; Rothberg, L. *Phys. Rev. Lett.* **2006**, *96*, 047403-1–047403-4.

(15) Farhat, H.; Son, H.; Samsonidze, G. G.; Reich, S.; Dresselhaus, M. S.; Kong, J. *Phys. Rev. Lett.* **2007**, *99*, 145506-1–145506-4.

(16) Araujo, P. T.; Doorn, S. K.; Kilina, S.; Tretiak, S.; Einarsson, E.; Maruyama, S.; Chacham, H.; Pimenta, M. A.; Jorio, A. *Phys. Rev. Lett.* **2007**, *98*, 067401-1–067401-4.

(17) Das, A.; Sood, A. K.; Govindaraj, A.; Saitta, A. M.; Lazzeri, M.; Mauri, F.; Rao, C. N. R. *Phys. Rev. Lett.* **2007**, 136803-1–136803-4.

(18) Wu, Y.; Maultzsch, J.; Knoesel, E.; Chandra, B.; Huang, M. Y.; Sfeir, M. Y.; Brus, L. E.; Hone, J.; Heinz, T. F. *Phys. Rev. Lett.* **2007**, *99*, 027402-1–027402-4.

(19) Kawamoto, H.; Uchida, T.; Kojima, K.; Tachibana, M. *J. Appl. Phys.* **2006**, *99*, 094309.

(20) Jiang, C. Y.; Kempa, K.; Zhao, J. L.; Schlecht, U.; Kolb, U.; Basche, T.; Burghard, M.; Mews, A. *Phys. Rev. B* **2002**, *66*, 161404-1–161404-4.

(21) Kempa, K. *Phys. Rev. B* **2002**, *66*, 195406-1–195406-5.

(22) Tsang, J. C.; Freitag, M.; Perebeinos, V.; Liu, J.; Avouris, P. *Nat. Nanotechnol.* **2007**, *2*, 725–730.

(23) Saito, R.; Jorio, A.; Hafner, J. H.; Lieber, C. M.; Hunter, M.; McClure, T.; Dresselhaus, G.; Dresselhaus, M. S. *Phys. Rev. B* **2001**, *64*, 085312-1–085312-7.

(24) Kim, Y. A.; Kojima, M.; Muramatsu, H.; Umemoto, S.; Watanabe, T.; Yoshida, K.; Sato, K.; Ikeda, T.; Hayashi, T.; Endo, M.; Terrones, M.; Dresselhaus, M. S. *Small* **2006**, *2*, 667–676.

(25) Kalbac, M; Kavan, L.; Zukalova, M; Dunsch, L. *Adv. Funct. Mater.* **2005**, *15*, 418–426.

(26) Kavan, L.; Dunsch, L. *Nano Lett.* **2003**, *3*, 969–972.

(27) Rafailov, P. M.; Thomsen, C.; Dettlaf-Weglikowska, U.; Hornbostel, B.; Roth, S. *Phys. Status Solidi B* **2007**, *244*, 4060–4063.

(28) Kalbac, M.; Kavan, L.; Zukalova, M.; Yang, S. F.; Cech, J.; Roth, S.; Dunsch, L. *Chem.—Eur. J.* **2007**, *13*, 8811–8817.

(29) Kataura, H.; Kumazawa, Y.; Maniwa, Y.; Umezu, I.; Suzuki, S.; Ohtsuka, Y.; Achiba, Y. *Synth. Met.* **1999**, *103*, 2555–2558.

(30) Kataura, H.; Maniwa, Y.; Kodama, T.; Kikuchi, K.; Hirahara, K.; Suenaga, K.; Iijima, S.; Suzuki, S.; Achiba, Y.; Kratschmer, W. *Synth. Met.* **2001**, *121*, 1195–1196.

NL073104H